

The structural and electronic properties of Ag-adsorbed $(\text{SiO}_2)_n$ ($n=1-7$) clusters

Gao-feng Zhao,^{a)} Li-li Zhi, and Ling-ju Guo

School of Physics and Electronics, Henan University, Kaifeng 475004, People's Republic of China

Zhi Zeng

Key Laboratory of Materials Physics, Institute of Solid State Physics, Chinese Academy of Sciences, Hefei 230031, People's Republic of China

(Received 11 September 2007; accepted 11 October 2007; published online 19 December 2007)

Equilibrium geometries, charge distributions, stabilities, and electronic properties of the Ag-adsorbed $(\text{SiO}_2)_n$ ($n=1-7$) clusters have been investigated using density functional theory with generalized gradient approximation for exchange-correlation functional. The results show that the Ag atom preferably binds to silicon atom with dangling bond in nearly a fixed direction, and the incoming Ag atoms tend to cluster on the existing Ag cluster leading to the formation of Ag islands. The adsorbed Ag atom only causes charge redistributions of the atoms near itself. The effect of the adsorbed Ag atom on the bonding natures and structural features of the silica clusters is minor, attributing to the tendency of stability order of $\text{Ag}(\text{SiO}_2)_n$ ($n=1-7$) clusters in consistent with silica clusters. In addition, the energy gaps between the highest occupied and lowest unoccupied molecular orbitals remarkably decrease compared with the pure $(\text{SiO}_2)_n$ ($n=1-7$) clusters, eventually approaching the near infrared radiation region. This suggests that these small clusters may be an alternative material which has a similar functionality in treating cancer to the large gold-coated silica nanoshells and the small $\text{Au}_3(\text{SiO}_2)_3$ cluster. © 2007 American Institute of Physics. [DOI: 10.1063/1.2805384]

I. INTRODUCTION

Silicon oxide is one of the most abundant materials on earth. Especially, silica has a wide range of application in microelectronics, optical communication, and thin-film technology. So interest in studying the properties of nanoparticles and clusters of silica is relatively recent.¹⁻³ On the other hand, silver, one of the noble metals, has practical importance because of its role in photography,⁴ catalysis,⁵ and its potential use in new electronic materials.⁶ Experimental evidence for the importance of the precise size of clusters deposited on a solid substrate has been found, for example, in the catalytic activity of gold clusters on oxide substrates⁷ and the minimum number of silver atoms to form an image speck.⁸ Theoretical interest in the bonding of metals on oxides have been reported, for example, the nucleation of small Cu clusters at the surface of silica.⁹ Also, cluster growth was observed for Au, Ag, and Cu deposited on C_{60} surface,¹⁰⁻¹⁵ and it is found that Ag donates electrons to the lowest unoccupied molecular orbital of C_{60} molecules resulting in a metallic conduction band.

One of the promising candidates to produce nonlinear optic devices is the nanocomposite system made of metal nanoclusters embedded in a dielectric matrix^{16,17} because of their fast response and strong nonlinear absorption.¹⁸ A large number of methods have been improved to obtain metal nanoclusters hosted in matrix for their chemical, catalytic,

and optical properties.^{19,20} A growing number of experimental and theoretical studies focus on the metal-SiO complexes. Köppe and Schaöckel²¹ recorded the IR spectra of M-SiO (M=Na, K) complexes in solid argon for the first time. Then, Mehner *et al.*²² showed that the Ag-SiO complex could be generated at low temperature. Moreover, the $\text{Ag}\cdots\text{SiX}$ (X=O, S) complexes had already been investigated by electron paramagnetic resonance spectroscopy.^{23,24}

Recently, it is interesting to notice that a new application of gold-coated silica nanoshells has been found in treating tumors and cancer.²⁵⁻²⁷ The nanoshell, consisting of a silica core of the order of 100 nm coated with about 20 nm of gold, could absorb near infrared light and convert light to heat, causing irreversible thermal cellular destruction. When the nanoshells were incorporated into human breast cells in the test tube, and then exposed to near infrared (NIR), 100% of the cancer cells were killed. So efforts have been made to understand the optical properties of gold-coated silica nanoshells using a simple model. It has been shown that the optical response is due to the hybridization of the surface plasmon of the inner and outer shells. Sun *et al.*²⁸ have studied the binding of gold atoms to a small silica cluster and shown that this small cluster can have a similar functionality in the treatment of cancer as the large size nanoshell. Furthermore, the enhanced Raman effect observed for adsorbates on silver surface seems to have a cluster counterpart.²⁹ Motivated by these findings, we have investigated the small silica cluster with the Ag atom to understand if such a small cluster has the particular optical property absorbing near infrared radiation. If so, what is the mechanism for such ad-

^{a)}Author to whom correspondence should be addressed. Fax: +86-378-3881602. Electronic mail: zgf@henu.edu.cn.

sorption, namely, how does the Ag atom bind to the $(\text{SiO}_2)_n$ ($n=1-7$) clusters? What effect does the Ag atom have on the electronic structure of silica cluster? In order to understand the optical property, we have to know the interaction between the Ag atom and silica cluster in detail.

In this paper, we have presented a systematic study of the equilibrium geometries, binding energies, electronic properties, and gaps between the highest occupied molecular orbital (HOMO) and the lowest unoccupied molecular orbital (LUMO). In the following section, the computational procedures employed in this work are briefly described followed by the results and discussion in the subsequent section.

II. COMPUTATIONAL DETAILS

All calculations are based on the density functional theory (DFT) in the DMOL³ package.^{30,31} In the electronic structure calculations, all electron treatment and double numerical basis including *d*-polarization function were chosen. The exchange-correlation interaction was treated within the generalized gradient approximation using PW91 functional. Self-consistent field calculations were done with a convergence criterion of 10^{-5} hartree on the total energy. The direct inversion in an iterative subspace approach was used to speed up self-consistent field convergence. In the geometry optimization, the converge thresholds were set to 0.002 hartree/Å for the forces, 0.005/Å for the displacement, and 10^{-5} hartree for the energy change. The on-site charges were evaluated via Mulliken population analysis.

To check the accuracy of exchange-correlation potentials and the basis set, we calculated the bond lengths for dimers of Ag_2 , AgSi , Si_2 , O_2 , and SiO . They are found to be 2.641, 2.475, 2.294, 1.225, and 1.530 Å, respectively, which are in good agreement with the experimental values of 2.530,³² 2.410,³³ 2.246, 1.210, and 1.510 Å.³⁴

III. RESULTS AND DISCUSSIONS

A. Structures and charge distributions

It has been well established that the ground state structures of $(\text{SiO}_2)_n$ clusters in the small size range ($n < 12$) are chainlike.³⁵⁻³⁸ In order to illustrate the effect of the adsorbed Ag atom on silica clusters, geometry optimizations of the $(\text{SiO}_2)_n$ ($n=1-7$) clusters are also calculated by using identical methods and basis sets. The ground state structures of silica cluster are in good agreement with the results calculated by Nayak *et al.*³⁵

To determine the ground state structures as well as the isomers of the AgSiO_2 , we have considered five different initial configurations to optimize. They are shown in Fig. 1(a), where the Ag atom was placed on different Si and O atoms in different directions. The geometry of SiO_2 is linear with a Si–O bond length of 1.53 Å, and the final optimized geometries of AgSiO_2 have two isomers, as shown in Fig. 1(b). The ground state configuration on the left has a C_{2v} planar geometry, which lies 0.072 eV lower in energy than the isomer on the right. In the ground state structure, two O atoms curve toward the Ag atom, on the contrary, two O atoms deviate from the Ag atom in the isomer.

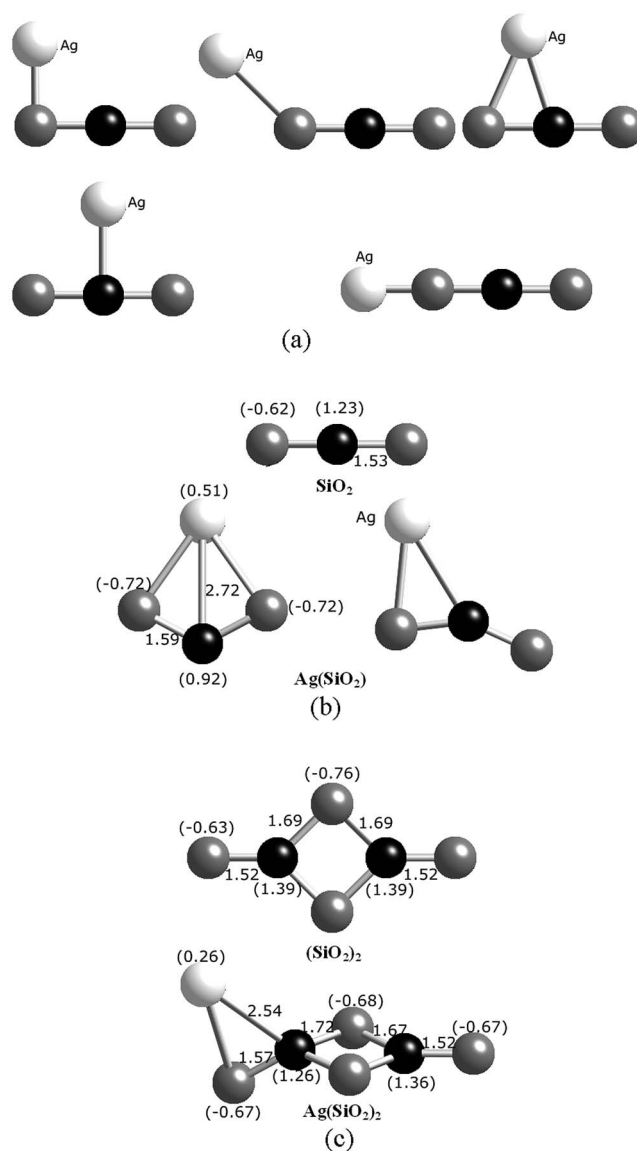


FIG. 1. (a) The initial configurations of AgSiO_2 . (b) Ground state structures of SiO_2 , AgSiO_2 , and the next higher energy isomers of AgSiO_2 . (c) Ground state structures of $(\text{SiO}_2)_2$ and $\text{Ag}(\text{SiO}_2)_2$. Mulliken charges given in parentheses and corresponding bond lengths are shown. Light color ball represents Ag atom, gray balls represent O atoms, and the black balls represent Si atom.

As a comparison, the pure $(\text{SiO}_2)_2$ cluster is also plotted in Fig. 1(c). It has a C_{2v} planar structure, then we have used several different initial configurations for optimizing the geometry, where the Ag atom was also placed on different Si and O atoms in $(\text{SiO}_2)_2$ cluster. Finally, these structures converged to the same one, as shown in Fig. 1(c). The Ag atom binds to one of the Si atoms, inducing the planar structure of $(\text{SiO}_2)_2$ cluster to three dimension. The corresponding bond length of Si–O, which is near the Ag atom, is increased from 1.52 to 1.57 Å. The Ag–Si bond length is 2.54 Å, and the angle ($\angle \text{AgSiSi}$) is 143.75° .

This trend continues as the size of $\text{Ag}(\text{SiO}_2)_n$ cluster increases. For $\text{Ag}(\text{SiO}_2)_3$ cluster, it is found that all the initial structures converge to the same one, as shown in Fig. 2. Here, the Ag atom also binds to one of the Si atoms at the end site. It is due to the fact that the middle Si atom is fully

TABLE I. $\text{Ag}(\text{SiO}_2)_n$ geometric parameters. Distances are in Å and angles are in deg. “outer” and “inner” refer to the site at the $(\text{SiO}_2)_n$ clusters.

Cluster	$r_{\text{Ag-Si}}$	$r_{\text{Si-O}}$ (outer)	$r_{\text{Si-O}}$ (inner)	$\angle(\text{AgSiSi})$	$\angle(\text{AgSiO})$ (outer)	$\angle(\text{AgSiO})$ (inner)
$\text{Ag}(\text{SiO}_2)$	2.72	1.59	1.59	61.84	61.84	
$\text{Ag}(\text{SiO}_2)_2$	2.54	1.57	1.72	143.75	69.11	125.60
$\text{Ag}(\text{SiO}_2)_3$	2.54	1.57	1.72	142.42	69.79	125.20
$\text{Ag}(\text{SiO}_2)_4$	2.54	1.57	1.72	148.82	68.91	125.88
$\text{Ag}(\text{SiO}_2)_5$	2.54	1.57	1.72	141.53	70.07	124.81
$\text{Ag}(\text{SiO}_2)_6$	2.54	1.57	1.72	142.85	69.38	125.38
$\text{Ag}(\text{SiO}_2)_7$	2.54	1.57	1.72	141.36	70.03	124.72

loses $1.23e$. When the Ag atom is attached on it, the number of electron lost by Si atom decreases to 0.92. Consequently, the Ag atom loses $0.51e$, and each O atom gets $0.72e$. In $(\text{SiO}_2)_2$, the two atoms at the end sites get about $0.63e$, and each of the double bridged O atoms gets $0.76e$, while each Si atom loses $1.39e$. The adsorption of the Ag atom causes redistribution of charges throughout the cluster. Two O atoms at end sites get $0.67e$. Each of the double bridged O atoms gets $0.68e$. While the Si atom near the Ag atom loses $1.26e$, the corresponding Ag atom loses $0.26e$.

From $n=3$ to $n=6$, it is shown that the electron number lost by the Ag atom is nearly a fixed value of 0.25. The small charge transfer suggests that there is a low covalent bonding between the Ag atom and silica clusters. The Si atom near the Ag atom loses about $1.21e$ on average, and one O atom at the end sites obtains about $0.67e$, corresponding to the value of 1.33 and 0.64 at the similar site in $(\text{SiO}_2)_n$ cluster. While the charge distributions of all the other atoms of Ag-adsorbed $(\text{SiO}_2)_n$ cluster are nearly invariable at the corresponding site compared with the silica cluster. It indicates that the Ag atom mainly causes the charge redistributions of the atoms near itself.

The electron configuration of the Ag atom, obtained from the natural bonding orbital analysis study, is listed in Table II. Generally, the population of $4d$ orbital of the Ag atom is nearly closed shell occupied about 10 electrons. In average, there are about $0.15e$ transferred from $5s$ to $5p$ orbital, and the other electrons lost by $5s$ orbital are transferred to silica cluster. This natural population show that the most important contribution to the Ag–Si bonding is the donation of the silver $5s$ electron. A remarkable difference from the Au-adsorbed on silica clusters,²⁸ is that the Ag atom loses

TABLE II. The most favorable dissociation channel and the dissociation energies (E_d) (eV) (the adsorption energies), electron configurations for the Ag atom.

Cluster	Dissociation channel	E_d (eV)	Electron configuration
$\text{Ag}(\text{SiO}_2)$	$\text{Ag} + \text{SiO}_2$	1.29	$\text{Ag}[\text{core}]4d^{10.002}5s^{0.330}5p^{0.155}$
$\text{Ag}(\text{SiO}_2)_2$	$\text{Ag} + (\text{SiO}_2)_2$	1.18	$\text{Ag}[\text{core}]4d^{9.955}5s^{0.629}5p^{0.151}$
$\text{Ag}(\text{SiO}_2)_3$	$\text{Ag} + (\text{SiO}_2)_3$	1.14	$\text{Ag}[\text{core}]4d^{9.956}5s^{0.639}5p^{0.150}$
$\text{Ag}(\text{SiO}_2)_4$	$\text{Ag} + (\text{SiO}_2)_4$	1.13	$\text{Ag}[\text{core}]4d^{9.963}5s^{0.636}5p^{0.155}$
$\text{Ag}(\text{SiO}_2)_5$	$\text{Ag} + (\text{SiO}_2)_5$	1.12	$\text{Ag}[\text{core}]4d^{9.954}5s^{0.650}5p^{0.151}$
$\text{Ag}(\text{SiO}_2)_6$	$\text{Ag} + (\text{SiO}_2)_6$	1.11	$\text{Ag}[\text{core}]4d^{9.955}5s^{0.644}5p^{0.153}$
$\text{Ag}(\text{SiO}_2)_7$	$\text{Ag} + (\text{SiO}_2)_7$	1.11	$\text{Ag}[\text{core}]4d^{9.955}5s^{0.652}5p^{0.150}$

electron, in contrast to the fact that the Au atom gets $0.81e$. This is because the electronegativity of the Au atom is greater than that of the Ag atom.

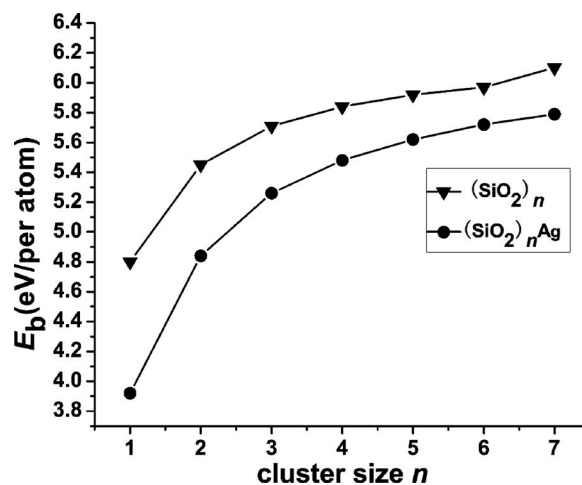
B. Stability

It is well known that the relative stability of the different sized clusters can be predicted by calculating the averaged binding energies and fragmentation energies. The averaged binding energies for $(\text{SiO}_2)_n$ and Ag-adsorbed $(\text{SiO}_2)_n$ ($n=1-7$) clusters can be defined by the following formula:

$$E_b(n) = \{nE(\text{Si}) + 2nE(\text{O}) - E[(\text{SiO}_2)_n]\}/3n, \quad (1)$$

$$E'_b(n) = \{nE(\text{Si}) + 2nE(\text{O}) + E(\text{Ag}) - E[\text{Ag}(\text{SiO}_2)_n]\}/3n + 1, \quad (2)$$

where E represents the total energy of the most stable $(\text{SiO}_2)_n$, $\text{Ag}(\text{SiO}_2)_n$, Si, O, and Ag clusters, respectively. The calculated results on the averaged binding energies are shown in Fig. 4. The averaged binding energies for $(\text{SiO}_2)_n$ and $\text{Ag}(\text{SiO}_2)_n$ clusters increase smoothly. It reflects that the stabilities of the clusters have been enhanced with the increase of cluster size. The predicted averaged binding energies of the $(\text{SiO}_2)_n$ cluster in this work are in good agreement with the previous calculated results.³⁵ It is noticed that the rate of the increase of the averaged binding energies for the two species clusters is almost the same.

FIG. 4. The averaged binding energies vs the size of $\text{Ag}(\text{SiO}_2)_n$ and $(\text{SiO}_2)_n$ clusters.

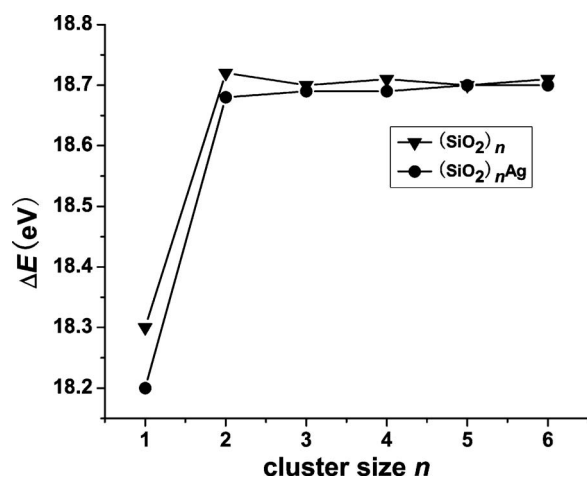


FIG. 5. The first order energy difference vs the size of $\text{Ag}(\text{SiO}_2)_n$ and $(\text{SiO}_2)_n$ clusters.

The relative stabilities of these clusters can be better understood by calculating the energy gained by increasing a SiO₂ unit to the clusters. We define $\Delta E(n)$ by the following formula:

$$\Delta E(n) = E(n) - E(n+1), \quad n \geq 1. \quad (3)$$

As shown in Fig. 5, the energy gain in adding a SiO₂ unit to the two species clusters increases dramatically from $n=1$ to $n=2$, but then remains nearly a constant as the clusters grow. Except for this sharp increase, the first energy difference $\Delta E(n)$ shows on conspicuous peaks. The trend is homologous between Ag-adsorbed $(\text{SiO}_2)_n$ clusters and pure $(\text{SiO}_2)_n$ clusters, which indicates the effect of the Ag atom to the bonding natures of silica clusters is small. This is in sharp contrast to metal-doped silicon clusters where binding energies evolve nonmonotonically and simultaneously many magic features are exhibited, presenting that some clusters are found to be more stable than others. This indicates that the natures of bonding between Si and SiO₂ clusters are different.

In order to investigate the stability of Ag-adsorbed silica clusters with the variation of size, it is necessary to calculate the fragmentation energies. The fragmentation energies can be defined by the following formula:

$$D(n) = E[\text{Ag}(\text{SiO}_2)_{n-1}] + E(\text{SiO}_2) - E[\text{Ag}(\text{SiO}_2)_n]. \quad (4)$$

As shown in Fig. 6, the fragmentation energies abruptly increase from $n=1$ to $n=2$. However, from $n=2$, the fragmentation energies increase, then nearly remain a constant value as the cluster grows, indicating that these clusters (from $n=2$ to $n=7$) have the same stability order. This also supports our stability consideration discussed above.

On the other hand, an interesting issue of this work is the dissociation products of the clusters, which is useful in vapor deposition or adatom adsorption on surfaces.⁴⁴ The most possible dissociation channels of the clusters considered as well as the corresponding dissociation are given in Table II. The dissociation energies of the favorable dissociation channel, namely,

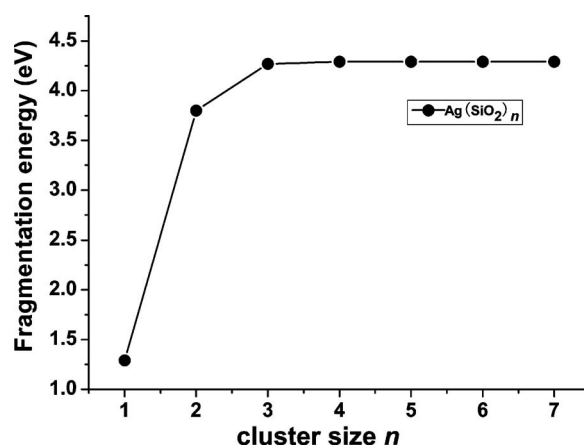


FIG. 6. The fragmentation energies vs the size of $\text{Ag}(\text{SiO}_2)_n$ clusters.



are defined by the following formula:

$$E = E(A_m) + E(B_n) - E(A_m B_n). \quad (6)$$

The most favorable dissociation channel for the $\text{Ag}(\text{SiO}_2)_n$ ($n=1-7$) cluster contains $(\text{SiO}_2)_n$ as a fragment, suggesting that the chainlike $(\text{SiO}_2)_n$ are more stable, which is in good agreement with the previous work.³⁵ The adsorption process is a converse process of the dissociation. In addition, the dissociation energies decrease with increasing the size of cluster and then remain a constant, suggesting that the energies needed to absorb a Ag atom are smaller with increasing the size of cluster in favor of size selectivity. It indicates that the Ag atom is more easily adsorbed on the silica cluster as the size increases. However, the adsorption energies are found to be 1.11–1.29 eV, suggesting the binding is strong. It may be a potential complex as a model metal-semiconductor system.

C. Ionization potentials and electron affinities

The vertical ionization potentials (VIPs) and the electron affinities (EAs) are obtained from

$$E_{\text{VIP}} = E_n^+ - E_n, \quad (7)$$

$$E_{\text{EA}} = E_n - E_n^-, \quad (8)$$

where E_n^+ and E_n^- are the total energies of the ionic clusters at the neutral optimized geometry. The vertical ionization potentials and electron affinities as a function of cluster size for $\text{Ag}(\text{SiO}_2)_n$ ($n=1-7$) clusters are shown in Fig. 7. It is observed that the values of the VIP decrease with the increase of the cluster size, in contrast, the values of electron affinities increase, except for $\text{Ag}(\text{SiO}_2)_5$ cluster. This is because that the vertical ionization potential of $(\text{SiO}_2)_5$ cluster is larger than that of its neighbors. Such feature is in good agreement with the theoretical results of Nayak *et al.*³⁵ Furthermore, it is observed that the VIP of the clusters varies from 8.03 to 8.72 eV, and the EA ranges from 1.60 to 2.74 eV. Clearly, the VIP is always larger than the EA for each considered isomer, implying that it is easier to gain an electron to the cluster than to remove an electron from the cluster.

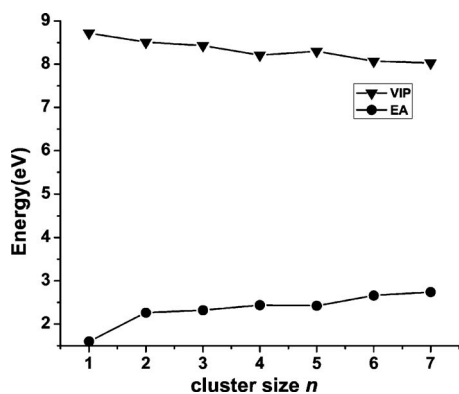


FIG. 7. The vertical ionization potentials and electron affinities vs the size of $\text{Ag}(\text{SiO}_2)_n$ clusters.

D. HOMO-LUMO gaps

An important electronic property of a cluster is the energy gap between HOMO and LUMO orbitals. As shown in Fig. 8, the HOMO-LUMO gaps become remarkably narrow compared with pure $(\text{SiO}_2)_n$ ($n=1-7$) cluster. The gap of the pure $(\text{SiO}_2)_n$ cluster ranges from 3.93 to 4.65 eV. When a single Ag atom is adsorbed, the gap is reduced to the range from 1.23 to 0.76 eV. Moreover, from $n=2$, the HOMO-LUMO gap of the Ag-adsorbed silica is relatively insensitive to the cluster size, namely, 0.76–0.78 eV, which corresponds to the NIR radiation region. This result strongly enhances our previous prediction, that is to say, such a small cluster can absorb near infrared radiation.

The optical adsorption of Ag-adsorbed silica cluster agrees very well with that of $\text{Au}_3(\text{SiO}_2)_3$ cluster calculated by Sun *et al.*²⁸ Through the time-dependent DFT calculation, they have studied the effect of gold coating on the optical properties of the nanosilica cluster. They recorded that the optical adsorption in $\text{Au}_3(\text{SiO}_2)_3$ cluster is close to the NIR. The reason is that the optical gap is reduced to 0.52 eV when the third Au atom is attached on $(\text{SiO}_2)_3$ cluster. In the experiment, it has been found that when a 22 nm thick gold shell was coated on a 96 nm diameter silica core, the adsorption wavelength was found to be 700 nm.²⁷ Although our calculated optical response of the $\text{Ag}(\text{SiO}_2)_n$ cluster is also

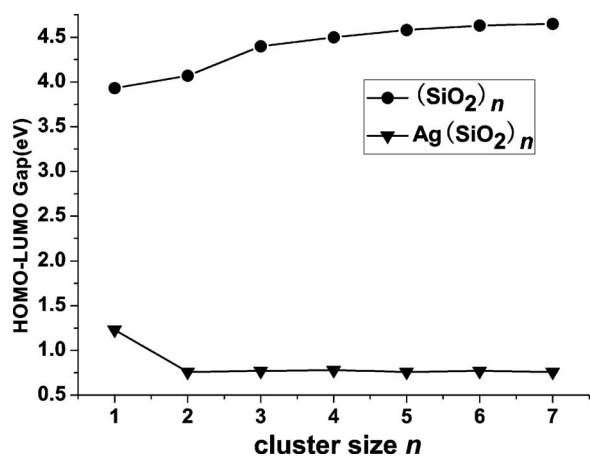


FIG. 8. The energy gap between HOMO and LUMO vs the size of $\text{Ag}(\text{SiO}_2)_n$ and $(\text{SiO}_2)_n$ clusters.

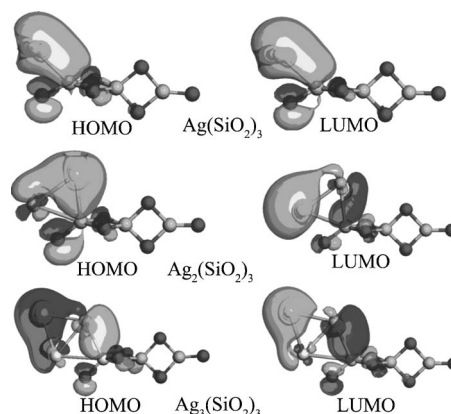


FIG. 9. HOMO and LUMO for $\text{Ag}(\text{SiO}_2)_3$, $\text{Ag}_2(\text{SiO}_2)_3$, and $\text{Ag}_3(\text{SiO}_2)_3$ clusters.

similar to that of the large nanoparticle, the mechanisms are entirely different. In the small clusters, the optical response is due to the interaction between the Ag atom and the silica cluster and the weak s - p hybridization of the Ag atom inducing the decrease of the HOMO-LUMO gaps, while in 100 nm size particle the optical response is due to the plasmon interaction.

However, the small cluster is superior to the large particle. One reason is that the small cluster may easily be penetrated in biological body such as cell and live tissues. The other one is the progression of synthetic technique in multicomponent clusters. Moreover, it is noted that in contrast with $\text{Au}_3(\text{SiO}_2)_3$ cluster, we need less Ag atoms to obtain a similar functionality in treating cancer. It suggests that the application of small Ag-adsorbed silica cluster may be more possible. So we can conclude that Ag-adsorbed silica cluster may be an alternative material in medicine.

In order to further probe the adsorption of many Ag atoms on silica, we have analyzed the electronic structure of $\text{Ag}(\text{SiO}_2)_3$, $\text{Ag}_2(\text{SiO}_2)_3$, and $\text{Ag}_3(\text{SiO}_2)_3$ clusters by studying the HOMO and LUMO. As shown in Fig. 9, we can see that the electron density is almost populating on the Ag atoms and these neighboring Si atoms, which indicates that the main contribution to these frontier orbital comes from the Ag atom and these neighboring atoms. This suggests that the incoming Ag atom will preferably bind with an existing Ag atom in the next growth stage. This has been actually happened, as shown in Fig. 2, where the second and the third Ag atoms both prefer to bind the first Ag atom. Such feature is different from that of the $\text{Au}-(\text{SiO}_2)_3$ cluster where the second Au atom is adsorbed on the Si atom at the other side of the $(\text{SiO}_2)_3$ cluster in Ref. 28. This seems to suggest that the tendency to form Ag islands is dependent not only on the dangling bonds but also on the distribution of the HOMO and LUMO.

IV. SUMMARY

In summary, we have calculated the geometrical and electronic structures of the Ag-adsorbed $(\text{SiO}_2)_n$ ($n=1-7$) clusters employing DFT with a generalized gradient correction to the exchange-correlation potential. The lowest energy structures, averaged binding energies, charge distribution,

vertical ionization potentials, electron affinities, and HOMO-LUMO gaps are obtained and compared with some experimental and previous theoretical conclusions. The main results can be summarized in the following points:

- (1) Owing to the dangling bonds, the single Ag atom preferably binds to one of the Si atom at the end site in a nearly fixed direction. The Ag atom primarily affects the charge redistribution of the atoms near itself.
- (2) According to the averaged binding energies, the first energy difference $\Delta E(n)$ and the fragmentation energies, we conclude that the averaged binding energies increase smoothly as the size of the (SiO₂)_n and Ag(SiO₂)_n ($n=1-7$) clusters increases. The same stability order of Ag(SiO₂)_n clusters from $n=2$ indicates that the effect of the Ag atom on the bonding natures of silica cluster is small.
- (3) Although the adsorbed Ag atom does not seriously distort the frames of pure silica clusters, the HOMO-LUMO gaps of the Ag(SiO₂)_n clusters decrease obviously as compared with silica clusters, corresponding to the NIR region. The reduction makes it possible to be another better material for treating cancer by absorbing near infrared light. In addition, we can conclude that the tendency to form Ag island is dependent not only on dangling bonds but also on the distribution of the HOMO and LUMO orbitals.

ACKNOWLEDGMENTS

The authors wish to thank Yuan-xu Wang for the helpful discussions. This work was supported by the National Science Foundation of China under Grant Nos. 10504036 and 90503005, the special Funds for Major State Basic Research Project of China(973) under Grant No. 2005CB623603, the Henan University National Science Foundation under Grant No. 06YBZR021, Knowledge Innovation Program of Chinese Academy of Sciences, and Director Grants of Hefei Institutes of Physical Sciences. Part of the calculations were performed in Center for Computational Science, Hefei Institutes of Physical Sciences.

¹L. S. Wang, J. B. Nicholas, M. Dupuis, H. Wu, and S. D. Colson, *Phys. Rev. Lett.* **78**, 4450 (1997).

²S. Li, S. J. Silvers, and M. S. El-Shall, *J. Phys. Chem. B* **101**, 1794 (1997).

³J. A. Harkless, D. K. Stlinger, and F. H. Stillinger, *J. Phys. Chem.* **100**, 1098 (1996).

⁴R. S. Eachus, A. P. Marchetti, and A. A. Muenter, *Annu. Rev. Phys. Chem.* **50**, 117 (1999).

⁵G. M. Koretsky and M. B. Knickelbein, *J. Chem. Phys.* **107**, 10555 (1997).

⁶S.-H. Kim, G. Medeiros-Ribeiro, D. A. A. Ohlberg, R. Stanley Williams, and J. R. Heath, *J. Phys. Chem.* **103**, 10341 (1999).

⁷A. Sanchez, S. Abbet, U. Heiz, W. D. Schneider, H. Hakkinen, R. N.

Barnett, and U. Landman, *J. Phys. Chem. A* **103**, 9573 (1999).

⁸P. Fayet, F. Granzer, G. Hegenbart, E. Moisar, B. Pischel, and L. Wöste, *Phys. Rev. Lett.* **55**, 3002 (1985).

⁹N. Lopez, F. Illas, and G. Pacchioni, *J. Phys. Chem. B* **103**, 1712 (1999).

¹⁰Y. Kuk, D. K. Kim, Y. D. Suh, K. H. Park, H. P. Noh, S. J. Oh, and S. K. Kim, *Phys. Rev. Lett.* **70**, 1948 (1993).

¹¹T. R. Ohno, Y. Chen, S. E. Harvey, G. H. Kroll, P. J. Benning, J. H. Weaver, L. P. F. Chibante, and R. E. Smalley, *Phys. Rev. B* **47**, 2389 (1993).

¹²J. E. Rowe, P. Rudolf, L. H. Tjeng, R. A. Malic, G. Meigs, C. T. Chen, J. Chen, and W. Plummer, *Int. J. Mod. Phys. B* **6**, 3909 (1992).

¹³D. Owens, C. Aldao, D. Poirier, and J. Weaver, *Phys. Rev. B* **51**, 17068 (1995).

¹⁴A. F. Hebard, R. R. Ruel, and C. B. Eom, *Phys. Rev. B* **54**, 14052 (1996).

¹⁵A. W. Dunn, B. N. Cotier, A. Nogaret, P. Moriarty, and P. H. Beton, *Appl. Phys. Lett.* **71**, 2937 (1997).

¹⁶V. Kreibig and M. Vollmer, *Optical Properties of Metal Clusters* (Springer, Berlin, 1995).

¹⁷P. Mazzoldi, G. W. Arnold, G. Battaglin, F. Gonella, and R. F. Haglund, Jr., *J. Nonlinear Opt. Phys. Mater.* **5**, 285 (1996).

¹⁸G. Yang, W. Wang, L. Yan, H. Lu, G. Yang, and Z. Chen, *Opt. Commun.* **209**, 445 (2002).

¹⁹M. Lee, T. S. Kim, and Y. S. Choi, *J. Non-Cryst. Solids* **211**, 143 (1997).

²⁰G. Compagnini, A. A. Scalisi, and O. Puglisi, *Phys. Chem. Chem. Phys.* **4**, 2787 (2002).

²¹R. Köppe and H. Schnöckel, *Heteroat. Chem.* **3**, 329 (1992).

²²T. Mehner, H. Schnöckel, C. Jouany, F. X. Gadea, and J. C. Barthelat, *Heteroat. Chem.* **3**, 333 (1992).

²³J. H. B. Chenier, J. A. Howard, H. A. Joly, B. Mile, and P. L. Timms, *J. Chem. Soc., Chem. Commun.* **1990**, 58.

²⁴J. A. Howard, R. Jones, J. S. Tse, M. Tomietto, P. L. Timms, and A. J. Seely, *J. Phys. Chem.* **96**, 9144 (1992).

²⁵L. R. Hirsch, R. J. Stafford, J. A. Bankson, S. R. Sershen, B. Rivera, R. E. Price, J. D. Hazle, N. J. Halas, and J. L. West, *Proc. Natl. Acad. Sci. U.S.A.* **100**, 13549 (2003).

²⁶M. Brongersma, *Nat. Mater.* **2**, 296 (2003).

²⁷L. R. Hirsch, J. B. Jackson, A. Lee, and N. J. Halas, *Anal. Chem.* **75**, 2377 (2003).

²⁸Q. Sun, Q. Wang, B. K. Rao, and P. Jena, *Phys. Rev. Lett.* **93**, 186803 (2004).

²⁹W.-T. Chan and R. Fournier, *Chem. Phys. Lett.* **315**, 257 (1999).

³⁰B. Delley, *J. Chem. Phys.* **92**, 508 (1990).

³¹B. Delley, *J. Chem. Phys.* **113**, 7756 (2000).

³²Y. Negishi, Y. Nakamura, and A. Nakajima, *J. Chem. Phys.* **115**, 3657 (2001).

³³J. J. Scherer, J. B. Paul, C. P. Collier, and R. J. Saykally, *J. Chem. Phys.* **103**, 113 (1995).

³⁴*CRC Handbook of Chemistry and Physics*, edited by D. R. Lide (CRC, Boca Raton, FL, 2000).

³⁵S. K. Nayak, B. K. Rao, S. N. Khanna, and P. Jena, *J. Chem. Phys.* **109**, 1245 (1998).

³⁶S. T. Bromley, M. A. Zwijnenburg, and Th. Maschmeyer, *Phys. Rev. Lett.* **90**, 035502 (2003).

³⁷Q. Sun, Q. Wang, and P. Jena, *Phys. Rev. Lett.* **92**, 039601 (2004).

³⁸J. Song and M. Choi, *Phys. Rev. B* **65**, 241302 (2002).

³⁹H. Häkkinen, M. Moseter, and U. Landman, *Phys. Rev. Lett.* **89**, 033401 (2002).

⁴⁰T. Nautiyal, S. J. Youn, and K. S. Kim, *Phys. Rev. B* **68**, 033407 (2003).

⁴¹E. M. Fernández, J. M. Soler, and L. C. Balbás, *Phys. Rev. B* **70**, 165403 (2004).

⁴²V. Bonačić-Koutecký, J. Burda, R. Mitrić, M. Ge, G. Zampella, and P. Fantucci, *J. Chem. Phys.* **117**, 3120 (2002).

⁴³H. M. Lee, M. Ge, B. R. Sahu, P. Tarakeshwar, and K. S. Kim, *J. Phys. Chem. B* **107**, 9994 (2003).

⁴⁴S. Erkoc, *Chem. Phys. Lett.* **369**, 605 (2003).